Gray spatial solitons in biased photorefractive media

Alexandra G. Grandpierre and Demetrios N. Christodoulides

Department of Electrical Engineering and Computer Science, Lehigh University, Bethlehem, Pennsylvania 18015

Tamer H. Coskun

Department of Electrical and Electronics Engineering, Pamukkale University, Denizli, Turkey

Mordechai Segev

Department of Physics, Technion—Israel Institute of Technology, Haifa 32000, Israel
and Department of Electrical Engineering, Princeton University, Princeton, New Jersey 08544

Yuri S. Kivshar

Optical Sciences Center, Research School of Physical Sciences and Engineering, Australian National University, Canberra ACT 0200, Australia

Received February 29, 2000; revised manuscript received September 11, 2000

We provide a detailed analysis of gray spatial optical solitons in biased photorefractive media. The properties associated with these solitons, such as their transverse velocity, spatial width, and phase profile, are obtained as functions of their normalized intensity and degree of "grayness." By employing the stability criterion based on the renormalized field momentum, we investigate the stability regions of gray spatial photorefractive solitons. The process of the soliton Y splitting arising from an initially even field depression is quasi-analytically described by use of a Hamiltonian formalism. © 2001 Optical Society of America

OCIS codes: 190.5330, 190.5530, 190.5940.

1. INTRODUCTION

During the past decade or so, dark optical solitons—both temporal and spatial—have been the focus of considerable attention.[1] In the spatiotemporal domain, dark optical solitons were first observed in low-loss optical fibers with normal dispersion.[2,3] Subsequently, dark spatial optical solitons were experimentally demonstrated in self-defocusing nonlinear media.[4–8] In this latter case a dark soliton or dark-soliton stripe (a dark notch or a void in intensity) forms when the effect of diffraction is exactly balanced by the self-defocusing nonlinearity of an optical medium. Thus far several physical systems have been identified as capable of supporting dark spatial solitons. These include Kerr media such as liquids, gases, and semiconductors as well as photorefractive crystals.[4–14]

The case of photorefractive solitons is of particular interest, since a photorefractive crystal does not resemble a Kerr material. In fact, photorefractive media are typically anisotropic, and their nonlinearity is nonlocal. Yet, as has been suggested theoretically, both bright and dark spatial solitons are possible in either biased photorefractives[15–18] or in crystals with appreciable photovoltaic coefficients.[19–21] The existence of steady-state photorefractive spatial solitons was successfully demonstrated in a series of experimental studies.[22] In particular, dark spatial solitons in the form of dark stripes or vortices have been observed in reverse-biased strontium barium niobate photorefractive crystals and photovoltaic lithium niobate samples.[9–14] In all of these cases, the observation of dark solitons was possible at relatively low power levels. Moreover, it was shown that their soliton-induced waveguides are capable of guiding other, more powerful beams at less-photosensitive wavelengths.[23]

One of the most interesting features of a dark-soliton beam is its ability to display a splitting behavior during propagation.[12,24–27] Depending on its input amplitude–phase profile, a dark beam can split into a sequence of dark or gray solitons. For example, under appropriate initial conditions, a dark beam can generate an odd number of dark depressions, provided its phase has a π phase jump at the input (odd phase profile),[28–30] or it may exhibit a more complicated splitting behavior in a general case.[31] When the phase jump is exactly π, the beam at the center forms a dark (black) soliton, whereas the remaining depressions represent pairs of gray solitons traveling in opposite directions. If, on the other hand, the input phase is constant across the dark beam (even phase profile), an even number of gray solitons emerge.[27–29] In this latter case pairs of gray solitons are generated and travel in opposite transverse directions so as to conserve the overall linear momentum of the system. This soliton Y splitting process, which is unique to dark-soliton beams, has been successfully used to write permanent

0740-3224/2001/010055-09$15.00 © 2001 Optical Society of America

Y-junction waveguide structures (3 dB splitters) in the bulk of a photorefractive crystal.[32,33] Such Y junctions can then be employed to guide signal (or probe) beams at less-photosensitive wavelengths ($\sim$1.5 μm) and can be permanently impressed or fixed into the crystalline lattice. Clearly, an investigation of the properties of these soliton-induced Y-junction photorefractive waveguides requires an in-depth understanding of the underlying soliton splitting dynamics. It is important to emphasize that, even though gray solitons were previously considered within the context of saturable Kerr nonlinearities,[4] the case of gray photorefractive solitons is by nature more complicated and so far has remained unexplored. To be more specific, dark beams in biased photorefractive crystals are governed by a nonlinear Schrödinger equation of the saturable type, which directly involves the boundary conditions of the space-charge field through the so-called $(1 + \rho)$ factor.[16–18] This, in turn, has important implications for the properties or characteristics of these photorefractive gray-soliton states. In this paper we provide a detailed analysis of gray spatial optical solitons in biased photorefractive media. The properties of these gray-soliton states, such as their transverse velocity, spatial width, and phase profile, are obtained as functions of their normalized intensity and their degree of grayness. In a certain range of the soliton parameters we find that the soliton total phase shift exceeds π, i.e., they become "darker than black."[34] Moreover, by employing the stability criterion based on the renormalized momentum,[35,36] we investigate the stability properties of gray photorefractive solitons. The Y soliton splitting arising from an initially even field depression is also semianalytically described by use of a Hamiltonian formalism and the associated conserved quantities. This, in turn, allows one to predict the Y-splitting angle and the grayness of the generated soliton pair once the parameters of the even field depression have been specified.

2. PROBLEM FORMULATION: DEFINITIONS

We start our analysis by considering a planar (stripe) optical beam propagating in a photorefractive material along the z axis. Being planar, the beam is allowed to diffract only along the x direction. Without any loss of generality, let us assume that the photorefractive crystal considered here is strontium barium niobate (SBN), with its optical c axis oriented along the x coordinate. The optical beam is linearly polarized along x, and the external bias field is applied in the same direction. Under these conditions it can be directly shown that the slowly varying envelope ϕ of the optical beam obeys the following evolution equation[16–18]:

$$i\frac{\partial \phi}{\partial z} + \frac{1}{2k}\frac{\partial^2 \phi}{\partial x^2} - \frac{k_0}{2}(n_e{}^3 r_{33} E_{\mathrm{sc}})\phi = 0, \tag{1}$$

where E_{sc} is the space charge field induced in this photorefractive material, which under steady-state conditions is given by

$$E_{\mathrm{sc}} = E_0\left(\frac{I_\infty + I_d}{I + I_d}\right). \tag{2}$$

Here n_e is the unperturbed extraordinary index of refraction, $k_0 = 2\pi/\lambda_0$, $k = k_0 n_e$, and r_{33} is the electro-optic coefficient involved. Other quantities are $I = I(x, z)$, the power density of the optical beam; I_d, the dark irradiance of the crystal; and I_∞, the intensity of the wave away from the dark notch of the wave, i.e., $I_\infty = I(x \to \pm\infty)$. E_0 is the value of the space charge field at $x \to \pm\infty$. If the spatial extent of the optical beam's dark depression is much less than the x-width W of the photorefractive crystal, then $E_0 \simeq \pm V/W$, where V is the external bias voltage used. Corrections regarding this approximation ($E_0 \simeq V/W$) can be found in Appendix A. We also point out that the dark irradiance of the crystal I_d can be artificially elevated by proper illumination of the crystal as demonstrated in previous experimental studies.[12]

It proves more convenient to normalize Eq. (1) by adopting the following transformations and dimensionless coordinates: $\phi = (2\eta_0 I_d/n_e)^{1/2} U$, $\xi = k_0 n_e{}^3 r_{33}|E_0|(z/2)$, and $s = k_0 n_e{}^2 (r_{33}|E_0|/2)^{1/2} x$. In this case one obtains

$$i\frac{\partial U}{\partial \xi} + \frac{1}{2}\frac{\partial^2 U}{\partial s^2} + (1 + \rho)\frac{U}{1 + |U|^2} = 0, \tag{3}$$

where $\rho = I_\infty/I_d$ is the so-called intensity ratio of the dark beam at $x \to \pm\infty$ with respect to I_d and ξ and s are dimensionless coordinates. The envelope U has been scaled with respect to the dark irradiance with η_0 representing the free-space intrinsic impedance. It is important to note that in the case of dark beams the boundary conditions of the space-charge field are directly involved in the evolution equation through the $(1 + \rho)$ factor. In essence, the strength of the nonlinearity increases linearly with the dark intensity ratio ρ. In deriving Eq. (3) we have also implicitly assumed that E_0 is negative so that dark solitons can be supported through the induced self-defocusing nonlinearity.

Equation (3) can be further renormalized[1] by use of the following gauge transformation $U = \Psi \exp(i\xi)$, in which case it takes the form:

$$i\frac{\partial \Psi}{\partial \xi} + \frac{1}{2}\frac{\partial^2 \Psi}{\partial s^2} + \left[\frac{(1 + \rho)}{1 + |\Psi|^2} - 1\right]\Psi = 0. \tag{4}$$

Note that in Eq. (4) the nonlinear term goes to zero at $s \to \pm\infty$ for optical beams of the dark type, since $|\Psi|^2 \to \rho$ for $s \to \pm\infty$. It is straightforward to show that Eq. (4) can also be obtained from the following Lagrangian density:

$$L = \frac{i}{2}(\Psi\Psi_\xi{}^* - \Psi^*\Psi_\xi) + \frac{1}{2}\Psi_s\Psi_s{}^* + (|\Psi|^2 - \rho) + (1 + \rho)\ln\left[\frac{(1 + \rho)}{1 + |\Psi|^2}\right], \tag{5}$$

where Ψ^* is the complex conjugate of Ψ, $\Psi_\xi = \partial\Psi/\partial\xi$, etc. Similarly, this system can be described within a Hamil-

tonian formalism. In this case, Eqs. (3) and (4) can be derived from the Hamiltonian density:

$$\hat{H} = \frac{1}{2}|U_s|^2 + (1+\rho)\ln\left[\frac{(1+\rho)}{1+|U|^2}\right] + (|U|^2 - \rho), \quad (6)$$

where in Eq. (6) we have used the fact that $|\Psi|^2 = |U|^2$ and $|\Psi_s| = |U_s|$. One can also easily show that Eq. (3) exhibits the following conservation laws:

$$N = \int_{-\infty}^{\infty} ds(|U|^2 - \rho), \quad (7)$$

$$P = \frac{i}{2}\int_{-\infty}^{\infty} ds(U_s^* U - U^* U_s)\left(1 - \frac{\rho}{|U|^2}\right) = \frac{i}{2}\int_{-\infty}^{\infty} ds(U_s^* U - U^* U_s) - \rho \,\mathrm{Arg}\, U|_{-\infty}^{\infty}, \quad (8)$$

$$H = \int_{-\infty}^{\infty} ds\left\{\frac{1}{2}|U_s|^2 + (1+\rho)\ln\left[\frac{(1+\rho)}{1+|U|^2}\right] + (|U|^2 - \rho)\right\}, \quad (9)$$

where N is related to the complementary power conveyed by the optical beam, P is the so-called renormalized momentum of the system, and H is the renormalized Hamiltonian. All three quantities, N, P, and H are finite because of this renormalization procedure, and, of course, they remain invariant during beam propagation. In what follows, the gray soliton solutions of Eq. (3) will be obtained.

3. PROPERTIES OF GRAY PHOTOREFRACTIVE SOLITONS

Before considering the gray-soliton solution of Eq. (3), it is useful to point out its Galilean invariance. In other words, one can show that after introduction of the transformation

$$U(s, \xi) = A(\eta,\zeta)\exp(i\alpha\eta)\exp(i\lambda\zeta) \quad (10)$$

in Eq. (3) and the moving coordinates $\eta = s - v\xi$, $\zeta = \xi$, the new envelope $A(\eta,\zeta)$ satisfies the same evolution equation [that is Eq. (3) governing U],

$$i\frac{\partial A}{\partial \zeta} + \frac{1}{2}\frac{\partial^2 A}{\partial \eta^2} + (1+\rho)\frac{A}{1+|A|^2} = 0. \quad (11)$$

Equation (11) is true provided that the gauge parameters α and λ satisfy the conditions $\alpha = v$ and $\lambda = v^2/2$. In this new moving-coordinate system v plays the role of a normalized transverse soliton velocity. Because of this one-to-one correspondence, any solution of Eq. (11) automatically satisfies Eq. (3) and vice versa. It can be directly shown that the gray-soliton solutions of Eq. (11) are given by[17]

$$A = \rho^{1/2} y(\eta)\exp\left[i\mu\zeta - iJ\int_0^{\eta}\frac{d\eta'}{y^2(\eta')} + i\Phi_0\right], \quad (12)$$

where J is a constant, $y(\eta)$ is a normalized function ($|y(\eta)| \leqslant 1$), and Φ_0 is an arbitrary phase. By imposing the condition $J = v$, the solution for the U envelope now reads as

$$U = \rho^{1/2} y(\eta)\exp\left\{i\left(\mu + \frac{v^2}{2}\right)\zeta + iv\left[\eta - \int_0^{\eta}\frac{d\eta'}{y^2(\eta')}\right] + i\Phi_0\right\}. \quad (13)$$

The condition $J = v$ was intentionally employed so as the phase of this gray spatial soliton is constant when η or $s \to \pm\infty$, which is consistent with the excitation conditions right at the origin. The quantity $(\mu + v^2/2)$ in Eq. (13) represents a nonlinear shift in the propagation constant. By substituting Eq. (13) into Eq. (3) we find that the normalized field profile $y(\eta)$ satisfies the following ordinary differential equation:

$$\frac{d^2 y}{d\eta^2} - 2\mu y - \frac{v^2}{y^3} + (1+\rho)\frac{2y}{1+\rho y^2} = 0. \quad (14)$$

We now look for gray-soliton solutions by imposing the boundary conditions, $y(0) = \sqrt{m}$ and $y(\eta) = 1$ at $\eta = \pm\infty$. The m parameter ($0 < m < 1$) describes the soliton grayness, i.e., the intensity at the middle of the wave defined as $I(0) = mI_{\infty}$.

Equation (14) can be easily integrated once (by quadrature), leading to

$$\frac{(y')^2}{2} - \mu y^2 + \frac{v^2}{2y^2} + \frac{(1+\rho)}{\rho}\ln(1+\rho y^2) = C, \quad (15)$$

where $y' = dy/d\eta$ and C is an integration constant. By applying the boundary conditions at $\eta \to \pm\infty$ and at $\eta = 0$, one can determine the parameters μ, v, and C. With the conditions $y = 1$ and $y' = y'' = 0$ at $\eta \to \pm\infty$, and $y^2(0) = m$, $y'(0) = 0$, we get

$$C = -\mu + \frac{v^2}{2} + \frac{(1+\rho)}{\rho}\ln(1+\rho), \quad (16)$$

$$C = -\mu m + \frac{v^2}{2m} + \frac{(1+\rho)}{\rho}\ln(1+m\rho), \quad (17)$$

$$v = [2(1-\mu)]^{1/2}, \quad (18)$$

from which the parameter μ can be determined, i.e.,

$$\mu = \frac{1}{1-m} + \frac{m}{(1-m)^2}\frac{(1+\rho)}{\rho}\ln\left(\frac{1+m\rho}{1+\rho}\right). \quad (19)$$

Thus, given the grayness m of this gray spatial soliton as well as its maximum intensity ratio ρ, one can then uniquely determine the parameter μ from Eq. (19) and, in turn, its transverse velocity v from Eq. (18) and C from either Eqs. (16) or (17). From here one can obtain the normalized field profile $y(\eta)$ by numerically integrating Eq. (15).

Figure 1(a) shows the normalized intensity of a gray photorefractive spatial optical soliton as a function of s for different values of the grayness parameter m when ρ

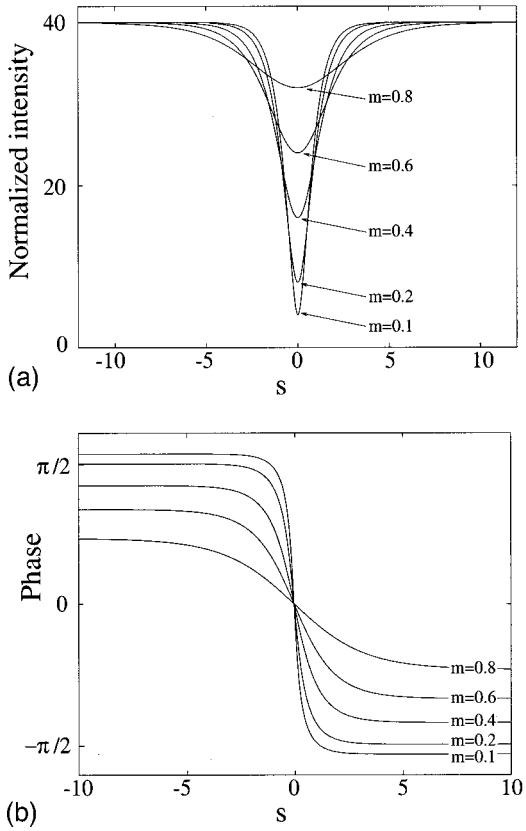

Fig. 1. (a) Normalized intensity profile of a gray photorefractive soliton at $\rho = 40$ and for various values of the grayness factor m; (b) associated phase profile of these gray solitons.

$= 40$. The associated soliton phase profiles are given in Fig. 1(b) for the same range of parameters. It is obvious from Fig. 1(a) that for a given intensity ratio the spatial soliton becomes narrower as m decreases (i.e., as the soliton becomes darker).

The normalized transverse velocity v is depicted in Fig. 2 as a function of ρ for various values of the grayness parameter m. As one can see, the normalized velocity v is bounded between 0 and 1. One can easily show from Eq. (19) that as $\rho \to 0$, $\mu \to 1$, and thus $v \to 0$. On the other hand, the same equation indicates that as $\rho \to \infty$ and $m \to 1$, the μ parameter approaches 1/2, and therefore $v \to 1$. Moreover, the normalized velocity quickly increases in the neighborhood of $\rho \approx 0$ and becomes almost constant at higher values of ρ ($\rho \gtrsim 40$). It is also interesting to note from Eqs. (18) and (19) that the soliton transverse velocity is approaching zero as $m \to 0$. This should have been anticipated, since this case corresponds to the fundamental dark (black) spatial soliton, the velocity of which is zero.

The normalized FWHM of the gray-soliton beam $\Delta\eta$ is shown in Fig. 3, where $\Delta\eta$ is defined as the spatial FWHM between the background and the lowest value of the intensity, i.e., the points where $y^2(\eta) = (1 + m)/2$. Figure 3 clearly indicates that the beam width generally decreases with the normalized intensity ratio ρ. At very low values of ρ (i.e., in the Kerr limit), $\Delta\eta$ decreases very rapidly, whereas it saturates for $\rho \gtrsim 40$. This saturation is predominantly due to the fact that the evolution equation itself involves the space-charge-field boundary conditions through the $(1 + \rho)$ factor. In fact, had this effect not been present, the FWHM curves would have behaved similarly to those of bright photorefractive solitons.[16–18] The beam width also increases with the degree of grayness m.

As noted above, the antisymmetric (with respect to η) phase profile of a gray photorefractive soliton is shown in Fig. 1(b). Of interest is the soliton total phase jump, i.e., the phase difference between the two infinite tails of the localized structure, shown in Fig. 4 for various values of ρ, m. As follows from this figure, this phase difference saturates at high values of ρ. Note that the phase jump exceeds π for relatively low degrees of grayness (when the soliton is close to being black). In essence, in this regime ($m \lesssim 0.2$) these gray spatial solitons can be called "darker than black," and similar results were previously found in the case of gray solitons in other saturable Kerr media.[34]

The angle θ at which a spatial dark soliton propagates with respect to the z axis is related to its transverse velocity v and in radians is given by

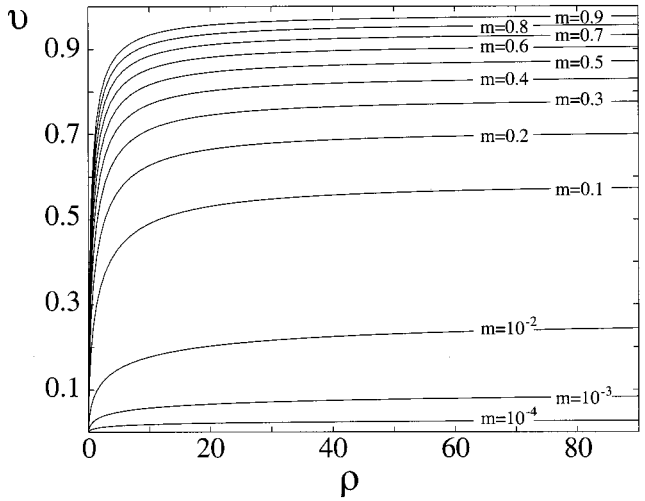

Fig. 2. Transverse velocity v of a gray photorefractive soliton as a function of ρ and m.

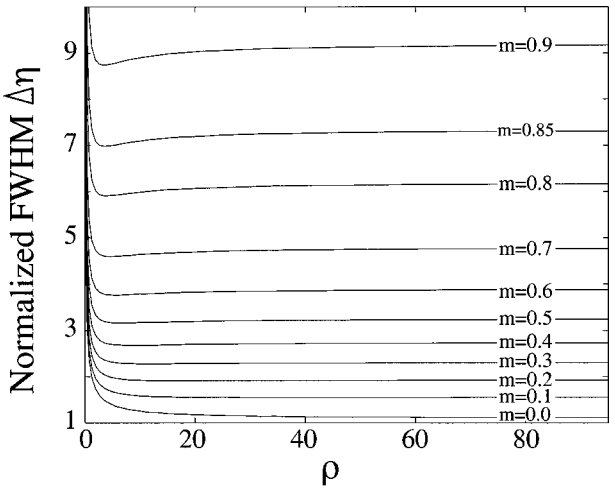

Fig. 3. Normalized FWHM of a gray photorefractive soliton as a function of ρ and m.

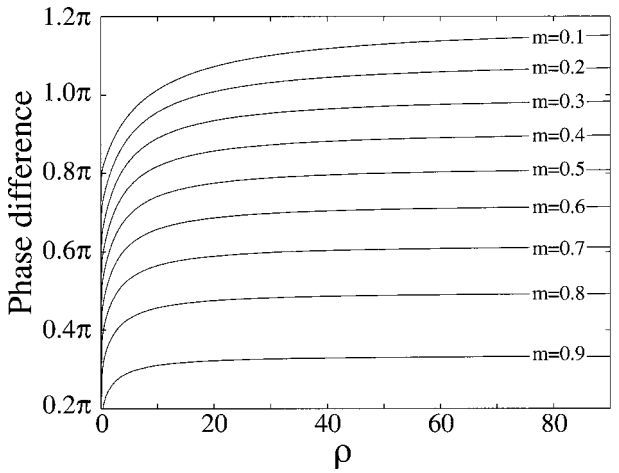

Fig. 4. Phase jump of a gray soliton as a function of ρ and m.

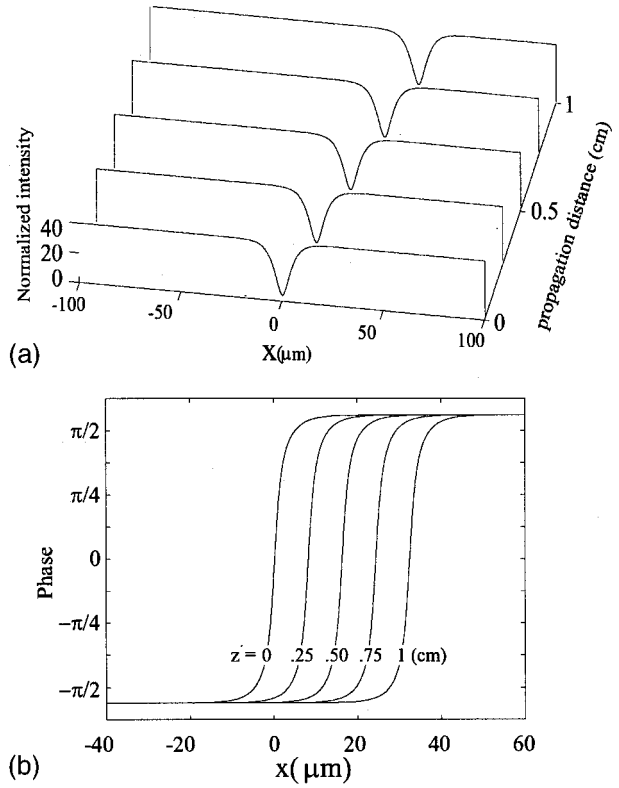

Fig. 5. (a) Normalized intensity and (b) phase profile of a gray photorefractive soliton propagating in a SBN crystal when $m = 0.1$ and $\rho = 40$.

$$\tan\,\theta = \frac{x}{z} = \frac{v}{\sqrt{2}} n_e (r_{33}|E_0|)^{1/2}. \tag{20}$$

To illustrate our results, let us consider as a first example a gray soliton of grayness $m = 0.1$ and background intensity ratio $\rho = 40$. Let the SBN crystal be 4.5 mm wide, $r_{33} = 280 \times 10^{-12}$ m/V, $n_e = 2.33$, and let the applied voltage be -200 V. The wavelength of the laser beam is 488 nm. Under these conditions one finds from Eq. (19) that $\mu = 0.84$ and, from Eq. (18), $v = 0.56$. The FWHM of the soliton spatial width can be deduced from Fig. 3 and in this case is $\Delta\eta \approx 1.6$ or, in real units, 9.2 μm. The angle of propagation is calculated to be 3.24 mrad, and after 1 cm of propagation the gray notch of the beam should be displaced by 32.4 μm. These analytical results are in agreement with numerical simulations, shown in Fig. 5(a), carried out by a beam propagation method. Figure 5(b) depicts the phase profile at each distance, where for demonstration we removed the phase term introduced by $(\mu + v^2/2)\xi$.

4. SOLITON Y-SPLITTING PROCESS

As previously discussed, under reverse bias, the soliton Y-splitting process can occur from an even field depression of a constant phase. Under appropriate initial conditions, such depressions split into two symmetric gray solitons, which propagate in opposite directions. In fact this Y splitting has been observed experimentally.[25,27] In what follows, we provide an approximate method that can semianalytically predict the properties and characteristics of the two gray photorefractive solitons generated during this Y-splitting soliton process.

Our approach is based on the total Hamiltonian H of the dynamical system defined by Eq. (9), which, as we know, remains invariant during propagation. If we now assume that the input is such that it eventually generates only two gray solitons (with very little radiation, if any), then the input Hamiltonian energy of the system will be equally divided between these two symmetric states. The reason we choose the Hamiltonian over the other two conserved quantities P, N is because the evolution equation itself [i.e., Eq. (3)] can be variationally derived from H. Therefore, to use this procedure, we must first find the static Hamiltonian H_s of a gray photorefractive soliton as a function of m, ρ. This Hamiltonian H_s can be obtained by substitution of Eq. (13) into Eq. (9), in which case one finds:

$$H_s = \int_{-\infty}^{\infty} ds \left\{ 2\rho(y^2 - 1) + 2(1 + \rho)\ln\left[\frac{(1 + \rho)}{1 + \rho y^2}\right]\right\}, \tag{21}$$

where $y(s)$ is the static field profile as obtained from Eq. (14). As a result, the Hamiltonian H_s is expected to de-

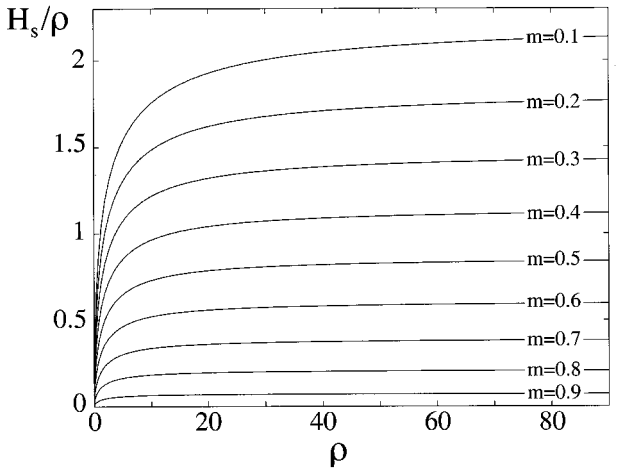

Fig. 6. Soliton Hamiltonian H_s/ρ as a function of ρ and m.

pend on both ρ,m. Figure 6 depicts the normalized Hamiltonian H_s/ρ of a photorefractive soliton [defined from Eq. (21)] as a function of both ρ and m.

Given an initially even field depression, one can obtain the total Hamiltonian H_i right at the input through Eq. (9). Since this Hamiltonian (or energy) of the system is conserved during evolution and is expected to be equally divided between the two gray photorefractive solitons, one can then determine the Hamiltonian of each component through $H_s = H_i/2$. Given the intensity ratio ρ involved in this photorefractive interaction, and since we now know H_s, the grayness m of each gray soliton can in turn be determined from Fig. 6. From here the normalized velocity v and the spatial FWHM $\Delta\eta$ can then be estimated with the help of Figs. 2 and 3, respectively. Finally, the actual Y-splitting angle can then be computed in radians through Eq. (20). Thus, given the initial field depression, all the relevant parameters involved in this Y-junction splitting process can be determined semianalytically from Figs. 2, 3, and 6. Conversely, one can solve the problem backwards. In other words, given the output data (the two gray solitons), one can determine the input depression and applied voltage required to lead to this interaction.

In the examples to follow, we consider even field depressions that are described by the analytical form $U(x, z = 0) = \rho^{1/2}[1 - \epsilon\mathrm{sech}^2(1.76x/x_0)]^{1/2}$, where x_0 is the spatial FWHM of the input, ϵ is associated with its grayness, and ρ is again the background intensity ratio. In all our examples, $\epsilon = 0.99$; that is, the input depression is almost black.

As a first example, let us consider soliton Y splitting in a SBN photorefractive crystal. The characteristics of the crystal are the same as those given in Section 3. Again $\lambda_0 = 488$ nm and the applied voltage is -200 V. The parameters of the even field depression at the input are $\rho = 40$ and $x_0 = 18$ μm. From these input data and Eq. (9) one finds that at $z = 0$ the normalized input Hamiltonian associated with the system is $H_i/\rho \approx 4.054$. Since the intensity ratio remains unchanged during propagation, the two gray solitons should also have $\rho = 40$. Furthermore, by assuming that the input "energy" is equally divided between the two components, the value of the Hamiltonian of each gray soliton is $H_s/\rho = H_i/2\rho \approx 2.027$. From Figs. 2, 3, and 6 one finds that the soliton grayness $m = 0.11$, the normalized velocity $v = 0.57$, and the actual intensity FWHM is 9.2 μm. From Eq. (20) the splitting angle is then found to be $\theta = 3.3$ mrad. We now check the accuracy of these semianalytical results by numerically solving Eq. (3) under the same initial conditions. Figure 7(a) shows the optical intensity during this Y-splitting process over a distance of 2.5 cm in this SBN crystal. The associated phase profile of these two gray solitons is also shown in Fig. 7(b). From these simulations we find that the intensity FWHM of each gray soliton is 9.3 μm, m is 0.12, and the splitting angle is asymptotically $\theta \approx 3.3$ mrad. These results are in excellent agreement with the predictions of our semianalytical approach.

As a second example, let us consider the same problem (the parameters of the problem are identical to those in the first example), but now the intensity FWHM of the in-

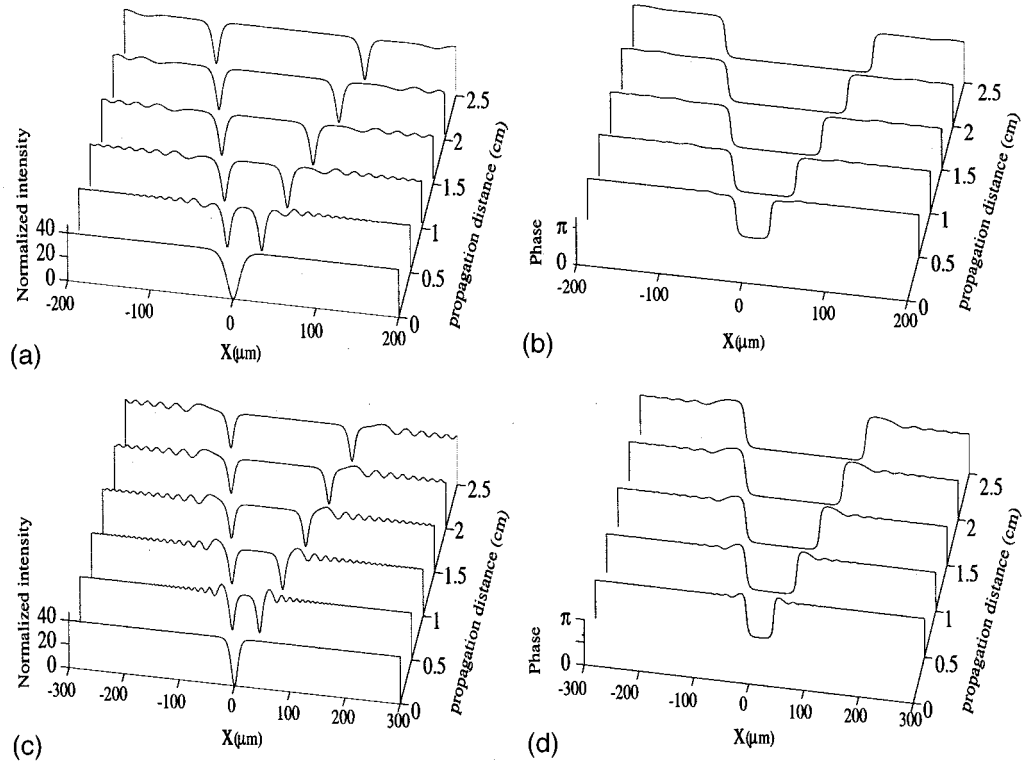

Fig. 7. (a) Normalized intensity and (b) corresponding phase profiles as obtained from numerical simulations of the soliton Y-splitting for $\rho = 40$ and when the spatial FWHM of the even field depression is $x_0 = 18$ μm. (c) Intensity and (d) phase profiles during Y-splitting in a SBN crystal when $\rho = 40$ and the initial FWHM of the even field depression is $x_0 = 14$ μm.

put depression is 14 μm. In this case $H_i/\rho = 3.34$. Following the same procedure as before, one finds that $H_s/\rho = H_i/2\rho \approx 1.67$ and hence $m = 0.22$, $v = 0.7$, and $\theta = 4.1$ mrad. The actual spatial FWHM of the two gray solitons is also found to be 11.1 μm. Figures 7(c) and 7(d) show the intensity and the phase profile, respectively, of this interaction as obtained from numerical simulations. From these numerical results we obtain $m = 0.25$ and $\theta = 4.3$ mrad, and the intensity FWHM of these states is 12 μm. Note that in this second example the error between the numerical and the semianalytical approaches has somewhat increased. The reason for such a discrepancy is related to the presence of radiative dispersive waves generated during the soliton splitting, as is clearly seen in Fig. 7(c). As a result, some part of the input Hamiltonian goes into these radiation components, and thus the condition $H_s = H_i/2$ is not exactly observed.

5. STABILITY OF GRAY PHOTOREFRACTIVE SOLITONS

It has been analytically and numerically demonstrated that dark or gray solitons described by the generalized nonlinear Schrödinger equations can be unstable[1,35,36] even though the nonlinearity is of the defocusing type. In these studies the criterion for dark soliton stability was found in terms of the derivative dP/dv, where P is the renormalized soliton momentum defined in Eq. (8) and v is the soliton normalized transverse velocity. More specifically, it was shown that when $dP/dv < 0$ a gray soliton is stable, whereas in the opposite case it is unstable.[1,35,36] In this section, we will employ this analytical criterion to determine whether gray photorefractive screening solitons are stable.

By substituting Eq. (13) into Eq. (8), one can find the renormalized momentum P_s for a gray photorefractive soliton:

$$P_s(v) = \rho v \int_{-\infty}^{\infty} ds \left[y(s) - \frac{1}{y(s)} \right]^2 . \qquad (22)$$

It is evident from Eq. (22) that the renormalized momentum is a function of both ρ and m. This dependence comes from the product ρv [through Eqs. (18) and (19)] and from the normalized field profile $y(s)$, which implicitly depends on this pair of variables [see Eq. (14)]. Figure 8(a) depicts the renormalized static momentum P_s/ρ of these gray photorefractive solitons for various values of the intensity ratio ρ and grayness m. On the other hand, Fig. 8(b) shows the renormalized momentum P_s/ρ as a function of velocity v for different values of ρ. As is clear from Fig. 8(b), for $\rho \lesssim 40$ the derivative dP_s/dv is always negative. However, for larger values of ρ the curve $P_s(v)$ attains a maximum. Thus photorefractive dark solitons for intensity ratios $\rho \gtrsim 40$ exhibit unstable regions for relatively small values of velocity v. In the unstable regions the same (P_s, ρ) can correspond to different values of v, which implies the existence of multivalued or multistable solutions.[35,36] It is interesting to note that in the regime examined ($0.01 \lesssim \rho \lesssim 1000$) the grayness parameter m of these unstable solutions happens to be rather small, i.e., they are almost black. For example, when ρ

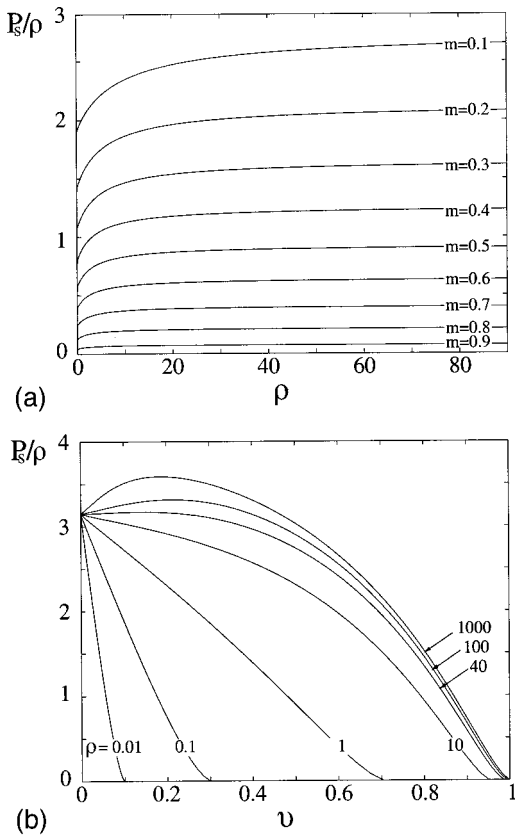

Fig. 8. (a) Renormalized momentum P_s/ρ of a dark or gray soliton as a function of ρ and m, (b) P_s/ρ as a function of v for various values of ρ.

$= 40$ and $v = 0.14$, $m = 3.8 \times 10^{-3}$. On the other hand, when $\rho = 100$ and $v = 0.22$, the grayness is $m = 8 \times 10^{-3}$.

Starting from Eq. (8), it is also straightforward to show that in the region $v \to 0$ (which corresponds to black solitons) the curves $P_s/\rho \to \pi$ for all values of the saturation parameter ρ.

This instability of gray photorefractive solitons is rather surprising, especially if one considers the $(1 + \rho)$ factor in Eq. (3), which tends to enhance the available nonlinearity in the system.

6. CONCLUSIONS

We have provided a comprehensive theoretical study of gray spatial optical solitons in biased photorefractive crystals. The properties of these gray solitons, such as their transverse velocity, spatial width, and phase profile, have been obtained as functions of their normalized intensity and degree of grayness. In a certain range of parameters, we have found that their total phase shift exceeds π, i.e., they become "darker than black" solitons. Moreover, by employing the soliton stability criterion based on the renormalized momentum, we have found that these gray photorefractive spatial solitons can be unstable for $\rho \gtrsim 40$. The soliton Y-splitting process arising from an initially even field depression has been also semianalytically described by means of a Hamiltonian technique.

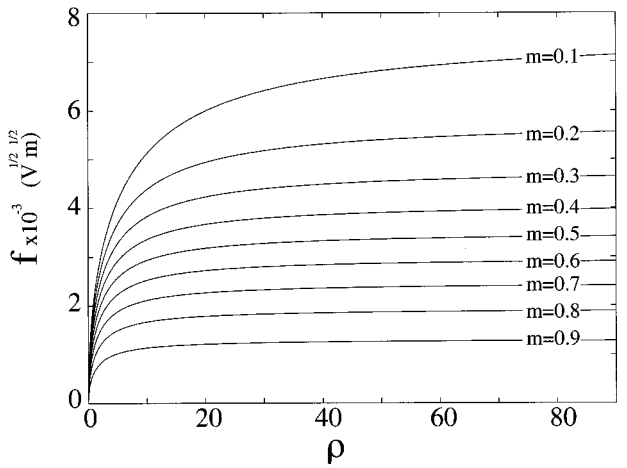

Fig. 9. Correction factor f for gray photorefractive solitons as a function of ρ and m.

APPENDIX A

The approximation $E_0 = V/W$ used in our analysis holds when the crystal width W is much larger than the soliton intensity FWHM. The correction factor f associated with this expression can be found for gray spatial solitons by a method similar to that used in Refs. 16 and 17. In this case we write $V = W|E_0| + f(|E_0|)^{1/2}$, from which one finds that

$$|E_0| = \left(\frac{-f + \sqrt{f^2 + 4W|V|}}{2W} \right)^2. \tag{A1}$$

It can then be shown that V and f are given by

$$|V| = 2\frac{|E_0|}{\alpha}\left[\int_0^{\hat{s}} \frac{(1+\rho)\mathrm{d}s}{(1+|U|^2)} + \left(\frac{\alpha W}{2} - \hat{s} \right) \right], \tag{A2}$$

where

$$\begin{aligned} f &= 2\frac{|E_0|^{1/2}}{\alpha}\int_0^{\hat{s}}\left[\frac{(1+\rho)\mathrm{d}s}{(1+|U|^2)} - \hat{s} \right] \\ &= 2\frac{|E_0|^{1/2}}{\alpha}\int_{\sqrt{m}}^{0.999}\left[\frac{(1+\rho)\mathrm{d}y}{(1+\rho y^2)y'} - \frac{\mathrm{d}y}{y'} \right], \end{aligned} \tag{A3}$$

$\alpha = (k_0{}^2 n_e{}^4 r_{33}|E_0|/2)^{1/2}$, and $\hat{s}$ is the half-spatial extent of these solitary waves for which $y^2(\hat{s}) = 0.999$. The correction factor f can be further evaluated in terms of ρ and m:

$$\begin{aligned} f = {} & \frac{(2|E_0|)^{1/2}}{\alpha}\int_{\sqrt{m}}^{0.999}\mathrm{d}y\left(\frac{1+\rho}{1+\rho y^2} - 1 \right) \\ & \times \left[\mu(y^2 - m) + (\mu - 1)\left(\frac{1}{y^2} - \frac{1}{m} \right) \right. \\ & \left. + \left(\frac{1+\rho}{\rho} \right)\ln\left(\frac{1+\rho m}{1+\rho y^2} \right) \right]^{-1/2}. \end{aligned} \tag{A4}$$

Figure 9 shows f (which is measured in units of $\mathrm{V}^{1/2}\,\mathrm{m}^{1/2}$) for various values of m and ρ, where the parameters used are identical to those employed to obtain Fig. 5, i.e., $|E_0| = 4.44 \times 10^4$ V/m, $\alpha = 1.74 \times 10^5\ \mathrm{m}^{-1}$. This correction factor is negligible when W is big enough, that is, for $f^2/(|V|W) \ll 1$ (Ref. 17), or $f \ll 1\ \mathrm{V}^{1/2}\,\mathrm{m}^{1/2}$. This is the case in the example depicted in Fig. 9.

ACKNOWLEDGMENTS

This work was supported by National Science Foundation (NSF), U.S. Air Force Office of Scientific Research, U.S. Army Research Office, U.S. Army Research Office Multidisciplinary University Research Initiative, and Australian Photonics Cooperative Research Center. The research of M. Segev was also supported by the fund for the Promotion of Research at the Technion.

REFERENCES

1. For a general overview, see Yu. S. Kivshar and B. Luther-Davies, "Dark optical solitons: physics and applications," Phys. Rep. **298**, 81–197 (1998).
2. P. Emplit, J. P. Hamaide, F. Reynaud, C. Froehly, and A. Barthelemy, "Picosecond steps and dark pulses through nonlinear single mode fibers," Opt. Commun. **62**, 374–379 (1987); D. Krökel, N. J. Halas, G. Giuliani, and D. Grischkowsky, "Dark-pulse propagation in optical fibers," Phys. Rev. Lett. **60**, 29–32 (1988).
3. A. M. Weiner, J. P. Heritage, R. J. Hawkins, R. N. Thurston, E. M. Kirschner, D. E. Leaird, and W. J. Tomlinson, "Experimental observation of the fundamental dark soliton in optical fibers," Phys. Rev. Lett. **61**, 2445–2448 (1988).
4. D. R. Andersen, D. E. Hooton, G. A. Swartzlander, Jr., and A. E. Kaplan, "Direct measurement of the transverse velocity of dark spatial solitons," Opt. Lett. **15**, 783–785 (1990).
5. G. A. Swartzlander, Jr., D. R. Andersen, J. J. Regan, H. Yin, and A. E. Kaplan, "Spatial dark-soliton stripes and grids in self-defocusing materials," Phys. Rev. Lett. **66**, 1583–1586 (1991).
6. S. R. Skinner, G. R. Allan, D. R. Andersen, and A. L. Smirl, "Dark spatial soliton propagation in bulk ZnSe," IEEE J. Quantum Electron. **27**, 2211–2219 (1991).
7. G. R. Allan, S. R. Skinner, D. R. Andersen, and A. L. Smirl, "Observation of fundamental dark spatial solitons in semiconductors using picosecond pulses," Opt. Lett. **16**, 156–158 (1991).
8. G. A. Swartzlander, Jr. and C. T. Law, "Optical vortex solitons observed in Kerr nonlinear media," Phys. Rev. Lett. **69**, 2503–2506 (1992).
9. G. Duree, M. Morin, G. Salamo, M. Segev, B. Crosignani, P. DiPorto, E. Sharp, and A. Yariv, "Dark photorefractive spatial solitons and photorefractive vortex solitons," Phys. Rev. Lett. **74**, 1978–1981 (1995); G. Duree, J. L. Shultz, G. Salamo, M. Segev, A. Yariv, B. Crosignani, P. DiPorto, E. Sharp, and R. R. Neurgaonkar, "Observation of self-trapping of an optical beam due to the photorefractive effect," Phys. Rev. Lett. **71**, 533–536 (1993).
10. M. Taya, M. C. Bashaw, M. M. Fejer, M. Segev, and G. C. Valley, "Observation of dark photovoltaic spatial solitons," Phys. Rev. A **52**, R3095–R3100 (1995).
11. M. D. Iturbe-Castillo, J. J. Sanchez-Mondragon, S. I. Stepanov, M. B. Klein, and B. A. Wechsler, "(1+1)-Dimension dark spatial solitons in photorefractive $Bi_{12}TiO_{20}$ crystal," Opt. Commun. **118**, 515–519 (1995).
12. Z. Chen, M. Mitchell, M.-F. Shih, M. Segev, M. H. Garrett, and G. C. Valley, "Steady-state dark photorefractive screening solitons," Opt. Lett. **21**, 629–631 (1996).
13. Z. Chen, M.-F. Shih, M. Segev, D. W. Wilson, R. E. Muller, and P. D. Maker, "Steady-state vortex-screening solitons formed in biased photorefractive media," Opt. Lett. **22**, 1751–1753 (1997).
14. Z. Chen, M. Segev, D. W. Wilson, R. E. Muller, and P. D.

Maker, "Self-trapping of an optical vortex by use of the bulk photovoltaic effect," Phys. Rev. Lett. **78**, 2948–2951 (1997).
15. M. Segev, B. Crosignani, A. Yariv, and B. Fischer, "Spatial solitons in photorefractive media," Phys. Rev. Lett. **68**, 923–926 (1992).
16. M. Segev, G. C. Valley, B. Crosignani, P. DiPorto, and A. Yariv, "Steady-state spatial screening solitons in photorefractive materials with external applied field," Phys. Rev. Lett. **73**, 3211–3214 (1994).
17. D. N. Christodoulides and M. I. Carvalho, "Bright, dark, and gray spatial soliton states in photorefractive media," J. Opt. Soc. Am. B **12**, 1628–1633 (1995).
18. M. Segev, M. F. Shih, and G. C. Valley, "Photorefractive screening solitons of high and low intensity," J. Opt. Soc. Am. B **13**, 706–718 (1996).
19. G. C. Valley, M. Segev, B. Crosignani, A. Yariv, M. M. Fejer, and M. Bashaw, "Dark and bright photovoltaic spatial solitons," Phys. Rev. A **50**, R4457–R4460 (1994).
20. M. Segev, G. C. Valley, M. Bashaw, M. Taya, and M. M. Fejer, "Photovoltaic spatial solitons," J. Opt. Soc. Am. B **14**, 1772–1781 (1997).
21. S. Bian, J. Frejlich, and K. H. Ringhofer, "Photorefractive saturable Kerr-type nonlinearity in photovoltaic crystals," Phys. Rev. Lett. **78**, 4035–4038 (1997).
22. M.-F. Shih, M. Segev, G. C. Valley, G. Salamo, B. Crosignani, and P. DiPorto, "Observation of two-dimensional steady-state photorefractive screening solitons," Electron. Lett. **31**, 826–827 (1995); M.-F. Shih, P. Leach, M. Segev, M. H. Garrett, G. Salamo, and G. C. Valley, "Two-dimensional steady-state photorefractive screening solitons," Opt. Lett. **21**, 324–326 (1996).
23. M. Morin, G. Duree, G. Salamo, and M. Segev, "Waveguides formed by quasi-steady-state photorefractive spatial solitons," Opt. Lett. **20**, 2066–2068 (1995).
24. B. Luther-Davies and Y. Xiaoping, "Waveguides and Y junctions formed in bulk media by using dark spatial solitons," Opt. Lett. **17**, 496–498 (1992).
25. Z. Chen, M. Mitchell, and M. Segev, "Steady-state photorefractive soliton-induced Y-junction waveguides and high-order dark spatial solitons," Opt. Lett. **21**, 716–718 (1996).
26. M. Taya, M. C. Bashaw, M. M. Fejer, M. Segev, and G. C. Valley, "Y junctions arising from dark-soliton propagation in photovoltaic media," Opt. Lett. **21**, 943–945 (1996).
27. Z. Chen, M. Segev, S. R. Singh, T. H. Coskun, and D. N. Christodoulides, "Sequential formation of multiple dark photorefractive spatial solitons: experiments and theory," J. Opt. Soc. Am. B **14**, 1407–1417 (1997).
28. V. E. Zakharov and A. B. Shabat, "Interaction between solitons in a stable medium," Sov. Phys. JETP **37**, 823–828 (1973).
29. K. J. Blow and N. J. Doran, "Multiple dark soliton solutions of the nonlinear Schrödinger equation," Phys. Lett. **107A**, 55–58 (1985).
30. G. P. Agrawal, *Nonlinear Fiber Optics*, 2nd ed. (San Diego, Academic Press, 1995).
31. A. N. Slavin, Yu. S. Kivshar, E. A. Ostrovskaya, and H. Benner, "Generation of spin-wave envelope dark solitons," Phys. Rev. Lett. **82**, 2583–2586 (1999).
32. M. Klotz, H. Meng, G. J. Salamo, M. Segev, and S. R. Montgomery, "Fixing the photorefractive soliton," Opt. Lett. **24**, 77–79 (1999).
33. M. Klotz, M. Crosser, G. J. Salamo, and M. Segev, "Fixing solitonic waveguides in photorefractive strontium barium niobate," *Technical Digest of the Topical Meeting on Nonlinear Guided Waves and Their Applications* (Optical Society of America, Washington, D.C., 1999), paper ThE8.
34. W. Królikowski, N. Akhmediev, and B. Luther-Davies, "Darker-than-black solitons: dark solitons with total phase shift greater than π," Phys. Rev. E **48**, 3980–3987 (1993).
35. Yu. S. Kivshar and W. Królikowski, "Instabilities of dark solitons," Opt. Lett. **20**, 1527–1529 (1995).
36. D. E. Pelinovsky, Yu. S. Kivshar, and V. V. Afanasjev, "Instability-induced dynamics of dark solitons," Phys. Rev. E **54**, 2015–2032 (1996); I. V. Barashenkov, "Stability criterion for dark solitons," Phys. Rev. Lett. **77**, 1193–1197 (1996).